

Measurement of $\psi(2S)$ Radiative Decays

M. Ablikim¹, J. Z. Bai¹, Y. Ban¹², X. Cai¹, H. F. Chen¹⁷, H. S. Chen¹, H. X. Chen¹, J. C. Chen¹, Jin Chen¹, Y. B. Chen¹, Y. P. Chu¹, Y. S. Dai¹⁹, L. Y. Diao⁹, Z. Y. Deng¹, Q. F. Dong¹⁵, S. X. Du¹, J. Fang¹, S. S. Fang^{1a}, C. D. Fu¹⁵, C. S. Gao¹, Y. N. Gao¹⁵, S. D. Gu¹, Y. T. Gu⁴, Y. N. Guo¹, Z. J. Guo^{16b}, F. A. Harris¹⁶, K. L. He¹, M. He¹³, Y. K. Heng¹, J. Hou¹¹, H. M. Hu¹, J. H. Hu³, T. Hu¹, G. S. Huang^{1c}, X. T. Huang¹³, X. B. Ji¹, X. S. Jiang¹, X. Y. Jiang⁵, J. B. Jiao¹³, D. P. Jin¹, S. Jin¹, Y. F. Lai¹, G. Li^{1d}, H. B. Li¹, J. Li¹, R. Y. Li¹, S. M. Li¹, W. D. Li¹, W. G. Li¹, X. L. Li¹, X. N. Li¹, X. Q. Li¹¹, Y. F. Liang¹⁴, H. B. Liao¹, B. J. Liu¹, C. X. Liu¹, F. Liu⁶, Fang Liu¹, H. H. Liu¹, H. M. Liu¹, J. Liu^{12e}, J. B. Liu¹, J. P. Liu¹⁸, Jian Liu¹, Q. Liu¹, R. G. Liu¹, Z. A. Liu¹, Y. C. Lou⁵, F. Lu¹, G. R. Lu⁵, J. G. Lu¹, C. L. Luo¹⁰, F. C. Ma⁹, H. L. Ma², L. L. Ma^{1f}, Q. M. Ma¹, Z. P. Mao¹, X. H. Mo¹, J. Nie¹, S. L. Olsen¹⁶, R. G. Ping¹, N. D. Qi¹, H. Qin¹, J. F. Qiu¹, Z. Y. Ren¹, G. Rong¹, X. D. Ruan⁴, L. Y. Shan¹, L. Shang¹, C. P. Shen¹, D. L. Shen¹, X. Y. Shen¹, H. Y. Sheng¹, H. S. Sun¹, S. S. Sun¹, Y. Z. Sun¹, Z. J. Sun¹, X. Tang¹, G. L. Tong¹, G. S. Varner¹⁶, D. Y. Wang^{1g}, L. Wang¹, L. L. Wang¹, L. S. Wang¹, M. Wang¹, P. Wang¹, P. L. Wang¹, Y. F. Wang¹, Z. Wang¹, Z. Y. Wang¹, Zheng Wang¹, C. L. Wei¹, D. H. Wei¹, Y. Weng¹, N. Wu¹, X. M. Xia¹, X. X. Xie¹, G. F. Xu¹, X. P. Xu⁶, Y. Xu¹¹, M. L. Yan¹⁷, H. X. Yang¹, Y. X. Yang³, M. H. Ye², Y. X. Ye¹⁷, G. W. Yu¹, C. Z. Yuan¹, Y. Yuan¹, S. L. Zang¹, Y. Zeng⁷, B. X. Zhang¹, B. Y. Zhang¹, C. C. Zhang¹, D. H. Zhang¹, H. Q. Zhang¹, H. Y. Zhang¹, J. W. Zhang¹, J. Y. Zhang¹, S. H. Zhang¹, X. Y. Zhang¹³, Yiyun Zhang¹⁴, Z. X. Zhang¹², Z. P. Zhang¹⁷, D. X. Zhao¹, J. W. Zhao¹, M. G. Zhao¹, P. P. Zhao¹, W. R. Zhao¹, Z. G. Zhao^{1h}, H. Q. Zheng¹², J. P. Zheng¹, Z. P. Zheng¹, L. Zhou¹, K. J. Zhu¹, Q. M. Zhu¹, Y. C. Zhu¹, Y. S. Zhu¹, Z. A. Zhu¹, B. A. Zhuang¹, X. A. Zhuang¹, B. S. Zou¹

(BES Collaboration)

¹ Institute of High Energy Physics, Beijing 100049, People's Republic of China

² China Center for Advanced Science and Technology(CCAST),
Beijing 100080, People's Republic of China

³ Guangxi Normal University, Guilin 541004, People's Republic of China

⁴ Guangxi University, Nanning 530004, People's Republic of China

⁵ Henan Normal University, Xinxiang 453002, People's Republic of China

⁶ Huazhong Normal University, Wuhan 430079, People's Republic of China

⁷ Hunan University, Changsha 410082, People's Republic of China

⁸ Jinan University, Jinan 250022, People's Republic of China

⁹ Liaoning University, Shenyang 110036, People's Republic of China

¹⁰ Nanjing Normal University, Nanjing 210097, People's Republic of China

¹¹ Nankai University, Tianjin 300071, People's Republic of China

¹² *Peking University, Beijing 100871, People's Republic of China*

¹³ *Shandong University, Jinan 250100, People's Republic of China*

¹⁴ *Sichuan University, Chengdu 610064, People's Republic of China*

¹⁵ *Tsinghua University, Beijing 100084, People's Republic of China*

¹⁶ *University of Hawaii, Honolulu, HI 96822, USA*

¹⁷ *University of Science and Technology of China, Hefei 230026, People's Republic of China*

¹⁸ *Wuhan University, Wuhan 430072, People's Republic of China*

¹⁹ *Zhejiang University, Hangzhou 310028, People's Republic of China*

^a *Current address: DESY, D-22607, Hamburg, Germany*

^b *Current address: Johns Hopkins University, Baltimore, MD 21218, USA*

^c *Current address: University of Oklahoma, Norman, Oklahoma 73019, USA*

^d *Current address: Universite Paris XI, LAL-Bat.*

208- BP34, 91898- ORSAY Cedex, France

^e *Current address: Max-Plank-Institut fuer Physik,
Foehringer Ring 6, 80805 Munich, Germany*

^f *Current address: University of Toronto, Toronto M5S 1A7, Canada*

^g *Current address: CERN, CH-1211 Geneva 23, Switzerland*

^h *Current address: University of Michigan, Ann Arbor, MI 48109, USA*

Abstract

Using 14 million $\psi(2S)$ events accumulated at the BESII detector, we report first measurements of branching fractions or upper limits for $\psi(2S)$ decays into $\gamma p\bar{p}$, $\gamma 2(\pi^+\pi^-)$, $\gamma K_S^0 K^+ \pi^- + c.c.$, $\gamma K^+ K^- \pi^+ \pi^-$, $\gamma K^{*0} K^- \pi^+ + c.c.$, $\gamma K^{*0} \bar{K}^{*0}$, $\gamma \pi^+ \pi^- p\bar{p}$, $\gamma 2(K^+ K^-)$, $\gamma 3(\pi^+ \pi^-)$, and $\gamma 2(\pi^+ \pi^-) K^+ K^-$ with the invariant mass of hadrons below $2.9 \text{ GeV}/c^2$. We also report branching fractions of $\psi(2S)$ decays into $2(\pi^+ \pi^-) \pi^0$, $\omega \pi^+ \pi^-$, $\omega f_2(1270)$, $b_1^\pm \pi^\mp$, and $\pi^0 2(\pi^+ \pi^-) K^+ K^-$.

PACS numbers: 13.20.Gd, 12.38.Qk, 14.40.Gx

Besides the conventional meson and baryon states, QCD also predicts a rich spectrum of glueballs, meson hybrids, and multi-quark states in the 1.0 to 2.5 GeV/c^2 mass region. Therefore, searches for the evidence of these exotic states play an important role to test QCD. Such studies have been performed in J/ψ radiative decays for a long time [1, 2], while studies in $\psi(2S)$ radiative decays have been limited due to low statistics in previous experiments [2, 3]. The radiative decays of $\psi(2S)$ to light hadrons are expected to contribute about 1% to the total $\psi(2S)$ decay width [4]. However, the measured channels only sum up to about 0.05% [3].

In this Letter, we present first measurements of $\psi(2S)$ decays into $\gamma p\bar{p}$, $\gamma 2(\pi^+\pi^-)$, $\gamma K_S^0 K^+\pi^- + c.c.$, $\gamma K^+ K^-\pi^+\pi^-$, $\gamma K^{*0} K^-\pi^+ + c.c.$, $\gamma K^{*0} \bar{K}^{*0}$, $\gamma \pi^+\pi^- p\bar{p}$, $\gamma 2(K^+ K^-)$, $\gamma 3(\pi^+\pi^-)$, and $\gamma 2(\pi^+\pi^-)K^+ K^-$, with the invariant mass of the hadrons (m_{hs}) less than 2.9 GeV/c^2 for each decay mode. Measurements of $\psi(2S)$ decays into $\pi^0 2(\pi^+\pi^-)$ and $\pi^0 2(\pi^+\pi^-)K^+ K^-$ are also presented and are used for estimating backgrounds contributing to $\psi(2S)$ decays into $\gamma 2(\pi^+\pi^-)$ and $\gamma 2(\pi^+\pi^-)K^+ K^-$, respectively.

The data samples used in this analysis consist of $(14.00 \pm 0.56) \times 10^6$ $\psi(2S)$ events ($\mathcal{L} = 19.72 \text{ pb}^{-1}$) and 6.42 pb^{-1} of continuum data at $\sqrt{s} = 3.65 \text{ GeV}$, acquired with the BESII detector. BESII is a conventional solenoid magnetic detector that is described in detail in Ref. [5]. A 12-layer vertex chamber (VC) surrounding the beam pipe provides trigger and track information. A forty-layer main drift chamber (MDC), located radially outside the VC, provides trajectory and energy loss (dE/dx) information for charged tracks over 85% of the total solid angle. The momentum resolution is $\sigma_p/p = 0.017\sqrt{1+p^2}$ (p in GeV/c), and the dE/dx resolution for hadron tracks is $\sim 8\%$. An array of 48 scintillation counters surrounding the MDC measures the time-of-flight (TOF) of charged tracks with a resolution of $\sim 200 \text{ ps}$ for hadrons. Radially outside the TOF system is a 12 radiation length, lead-gas barrel shower counter (BSC), which measures the energies of electrons and photons over $\sim 80\%$ of the total solid angle with an energy resolution of $\sigma_E/E = 22\%/\sqrt{E}$ (E in GeV). Outside of the solenoid coil, which provides a 0.4 Tesla magnetic field over the tracking volume, is an iron flux return that is instrumented with three double layers of counters that identify muons with momentum greater than $0.5 \text{ GeV}/c$.

In this analysis, a GEANT3 based Monte Carlo (MC) program with detailed consideration of the detector performance (such as dead electronic channels) is used to determine mass resolutions and detection efficiencies. The consistency between data and MC has been carefully checked in many high purity physics channels, and the agreement is reasonable [6].

A common set of requirements is used to select charged tracks and photon candidates for all channels. Each charged track is required to be well fitted to a helix in the MDC, to be within the polar angle region $|\cos\theta| < 0.8$, and to have a transverse momentum larger than $70 \text{ MeV}/c$. The total charge of the good charged tracks in each event is required to be zero. Each photon candidate is required to have an energy deposit in the BSC greater than 50 MeV , to be isolated from charged tracks by more than 15° , and to have the angle between the cluster development direction in the BSC and the photon emission direction less than 37° .

For each decay mode, the number of charged tracks is required to be equal to the number of charged stable hadrons in the corresponding final state. The TOF and dE/dx measurements of the charged track are used to calculate χ^2_{PID} values and the corresponding confidence levels (C.L.) for the hypotheses that the particle is a pion, kaon, or proton. All charged tracks in the selection of $\psi(2S) \rightarrow \gamma p\bar{p}$, $\gamma 2(\pi^+\pi^-)$, and $\gamma 2(K^+K^-)$ are required to be consistent with the proton, pion, or kaon assumption with the corresponding C.L. greater than 1%. For $\psi(2S) \rightarrow \gamma K^+K^-\pi^+\pi^-$, $\gamma\pi^+\pi^-p\bar{p}$, and $\gamma 2(\pi^+\pi^-)K^+K^-$, only two charged tracks are required to be identified as kaons or protons, respectively.

Next, the selected charged tracks and the photon with the largest energy are fitted kinematically using energy and momentum conservation constraints (4C), and the combined probability, $\text{prob}(\chi^2_{\text{com}}, \text{ndf})$ is required to be greater than 1%, where ndf is the number of degrees of freedom and χ^2_{com} is the sum of the χ^2 of the kinematic fit (χ^2_{4C}) and particle identification ($\chi^2_{\text{PID}}(i)$), *i.e.* $\chi^2_{\text{com}} = \sum_i \chi^2_{\text{PID}}(i) + \chi^2_{4C}$, where i runs over all charged tracks. For $\psi(2S) \rightarrow \pi^0 2(\pi^+\pi^-)$ and $\pi^0 2(\pi^+\pi^-)K^+K^-$, if there are more than two photons in an event, the photon-pair with the minimum χ^2_{com} is chosen. To remove background from charged particle misidentification, the χ^2_{com} for the signal hypothesis is required to be less than those for background.

To select $\gamma K_S^0 K^+\pi^- + c.c.$ events, the K_S^0 candidate must have a decay length in the transverse plane greater than 0.5 cm. In selecting $\psi(2S) \rightarrow \gamma K^+K^-\pi^+\pi^-$, contaminations from $\psi(2S) \rightarrow \gamma K_S^0 K\pi$ is removed by requiring the invariant mass of the two pions to be outside of the K_S^0 mass region, *i.e.*, $|m_{\pi\pi} - m_{K_S^0}| > 0.04 \text{ GeV}/c^2$.

To reject $\psi(2S)$ transitions into other charmonium states, m_{hs} is required to be less than 2.9 GeV/c^2 for each decay mode. If there is possible background from $\psi(2S) \rightarrow \pi^+\pi^-J/\psi$, it is removed by requiring $|m_{\text{recoil}}^{\pi^+\pi^-} - m_{J/\psi}| > 0.05 \text{ GeV}/c^2$, where $m_{\text{recoil}}^{\pi^+\pi^-}$ is the mass recoiling from each possible $\pi^+\pi^-$ pair.

Figure 1 shows invariant mass distributions of the hadrons for $\psi(2S) \rightarrow \gamma p\bar{p}$, $\gamma 2(\pi^+\pi^-)$, $\gamma K_S^0 K^+\pi^- + c.c.$, $\gamma K^+K^-\pi^+\pi^-$, $\gamma 2(K^+K^-)$, $\gamma\pi^+\pi^-p\bar{p}$, $\gamma 2(\pi^+\pi^-)K^+K^-$, and $\gamma 3(\pi^+\pi^-)$ below 2.9 GeV/c^2 , where backgrounds are shown as shaded histograms. The backgrounds of each decay mode fall into three classes: QED processes, estimated using the continuum data; multi-photon backgrounds, e.g. $\psi(2S) \rightarrow \pi^0 + \text{hadrons}$, $3\gamma + \text{hadrons}$, etc., where the *hadrons* have the same charged tracks as the signal final state, estimated with the MC simulation and normalized according to their branching fractions [3, 7, 8]; and other backgrounds, estimated using the inclusive $\psi(2S)$ decay MC sample [9]. The results show that the multi-photon backgrounds are dominant; the QED background, and the other backgrounds, including contamination between studied channels are lower. The observed χ^2_{4C} distributions include both signal events and these backgrounds (see Fig. 2).

The number of signal events is extracted by fitting the observed χ^2_{4C} distributions with those of the signal and background channels [10], *i.e.* $\chi^2_{\text{obs}} = w_s \chi^2_{\text{sig}} + \sum_{w_{b_i}} w_{b_i} \chi^2_{\text{bg}}$, where w_s and w_{b_i} are the weights of the signal and the background decays, respectively. As an example, Fig. 2 shows the χ^2 distribution observed for $\psi(2S) \rightarrow \gamma 2(\pi^+\pi^-)$, together with the fitted χ^2 distributions for the signal, multi-photon, QED, and other background channels.

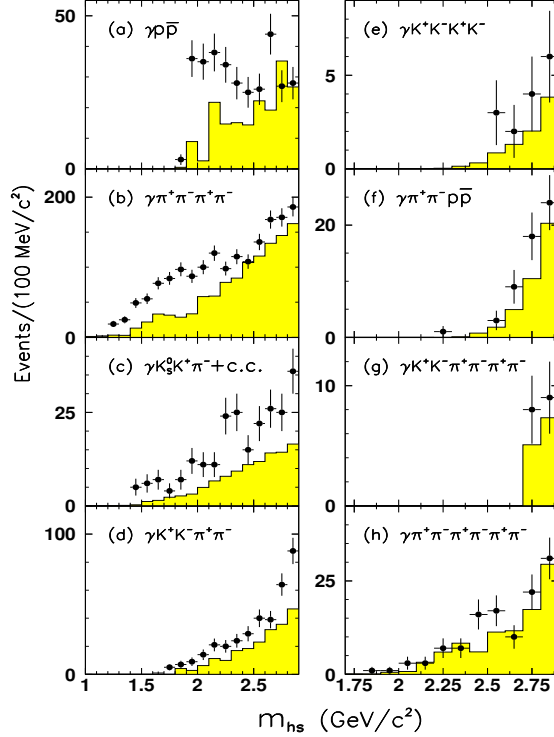


FIG. 1: Invariant mass distributions of the hadrons in each final state (dots with error bars). The shaded histograms are backgrounds.

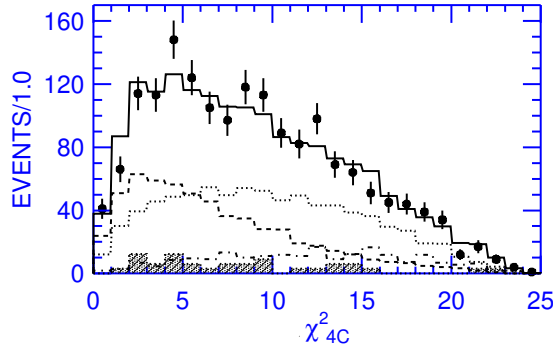


FIG. 2: The fitted χ^2_{4C} distribution for $\psi(2S) \rightarrow \gamma 2(\pi^+ \pi^-)$ candidate events. The dots with error bars are data. The solid line is the fitted result with the four components: signal events (dashed line), MC simulated multi-photon backgrounds (dotted line), QED processes (hatched histogram), and the other backgrounds (dot-dashed line).

In the fit, the weights of the multi-photon backgrounds and the QED backgrounds (w_b) are fixed to be the normalization factors, but the weight of the signal (w_s) and the weight of the other backgrounds (w_b) are free. With this method, the numbers of signal events are extracted for each decay mode with $m_{hs} < 2.9 \text{ GeV}/c^2$ and are listed in Table I.

In Fig. 1(a) there is an excess of events between $p\bar{p}$ threshold and $2.5 \text{ GeV}/c^2$, but no

TABLE I: Results for $\psi(2S) \rightarrow \gamma + \text{hadrons}$. For each final state, the following quantities are given: the number of events for $m_{hs} < 2.9 \text{ GeV}/c^2$ in $\psi(2S)$ data, N^{Tot} ; the number of background events from $\psi(2S)$ decays and QED processes, N^{Bg} ; the number of signal events, N^{Sig} ; and the weighted averaged efficiency, ϵ ; the branching fraction with statistical and systematic errors or the upper limit on the branching fraction at the 90% C.L. Possible interference effects for the modes with intermediate states are ignored.

| Mode | N^{Tot} | N^{Bg} | N^{Sig} | $\epsilon(\%)$ | $\mathcal{B}(\times 10^{-5})$ |
|----------------------------------|-----------|----------|--------------|----------------|-------------------------------|
| $\gamma pp\bar{p}$ | 329 | 187 | 142 ± 18 | 35.3 | $2.9 \pm 0.4 \pm 0.4$ |
| $\gamma 2(\pi^+\pi^-)$ | 1697 | 1114 | 583 ± 41 | 10.4 | $39.6 \pm 2.8 \pm 5.0$ |
| $\gamma K_S^0 K^+ \pi^- + c.c.$ | — | — | 115 ± 16 | 4.83 | $25.6 \pm 3.6 \pm 3.6$ |
| $\gamma K^+ K^- \pi^+ \pi^-$ | 361 | 229 | 132 ± 19 | 4.94 | $19.1 \pm 2.7 \pm 4.3$ |
| $\gamma K^{*0} K^+ \pi^- + c.c.$ | — | — | 237 ± 39 | 6.86 | $37.0 \pm 6.1 \pm 7.2$ |
| $\gamma K^{*0} \bar{K}^{*0}$ | 58 | 17 | 41 ± 8 | 2.75 | $24.0 \pm 4.5 \pm 5.0$ |
| $\gamma \pi^+ \pi^- pp\bar{p}$ | 55 | 38 | 17 ± 7 | 4.47 | $2.8 \pm 1.2 \pm 0.5$ |
| $\gamma K^+ K^- K^+ K^-$ | 15 | 8 | < 14 | 2.93 | < 4.0 |
| $\gamma 3(\pi^+\pi^-)$ | 118 | 95 | < 45 | 1.97 | < 17 |
| $\gamma 2(\pi^+\pi^-) K^+ K^-$ | 17 | 13 | < 15.5 | 0.69 | < 22 |

significant narrow structure due to the $X(1859)$ observed in $J/\psi \rightarrow \gamma pp\bar{p}$ [11]. A fit of the mass spectrum with an acceptance-weighted S -wave Breit-Wigner for the X resonance (with mass and width fixed to 1859 MeV/ c^2 and 30 MeV/ c^2 , respectively), together with MC simulated background channels along with $\psi(2S) \rightarrow \gamma pp\bar{p}$ phase space background [12] yields 11.7 ± 6.7 events with a statistical significance of 2.0σ . The upper limit on the branching fraction is determined to be $\mathcal{B}[\psi(2S) \rightarrow \gamma X(1859) \rightarrow \gamma pp\bar{p}] < 5.4 \times 10^{-6}$ at the 90% C.L.

There is a clear $K^{*0}(\bar{K}^{*0})$ signal in the $K\pi$ invariant mass spectrum for $\psi(2S) \rightarrow \gamma K^+ K^- \pi^+ \pi^-$ candidates. The $\psi(2S) \rightarrow \gamma K^{*0} K^- \pi^+ + c.c.$ and $\gamma K^{*0} \bar{K}^{*0}$ branching fractions are measured. The $\psi(2S) \rightarrow \gamma K^{*0} K^- \pi^+ + c.c.$ branching fraction includes the contribution from the $\psi(2S) \rightarrow \gamma K^{*0} \bar{K}^{*0}$, and the $\psi(2S) \rightarrow \gamma K^{*0} K\pi$ detection efficiency includes the effect of this contribution. Table I summarizes the branching fractions or upper limits for the $\psi(2S)$ radiative decays analyzed. We also report the differential branching fractions of $\psi(2S)$ decays into $\gamma pp\bar{p}$, $\gamma 2(\pi^+\pi^-)$, $\gamma K^+ K^- \pi^+ \pi^-$, and $\gamma K_S^0 K^+ \pi^- + c.c.$, as shown in Fig. 3.

For $\psi(2S)$ decays into $\pi^0 2(\pi^+\pi^-)$ and $\pi^0 2(\pi^+\pi^-) K^+ K^-$, the event selections are similar to those for $\psi(2S) \rightarrow \gamma 2(\pi^+\pi^-)$ and $\gamma 2(\pi^+\pi^-) K^+ K^-$, respectively, but two photons are required. The numbers of signal events are obtained by fitting the photon pair invariant mass distributions, and the results are listed in Table II. For $\psi(2S) \rightarrow \pi^0 2(\pi^+\pi^-)$ candidate events, intermediate resonances including σ [$f_0(600)$], $f_2(1270)$, ω , and $b_1(1235)$ are observed in the invariant mass distributions of two pions, three pions, and $\omega\pi$, as shown in Fig. 4. The results for these resonances are given in Table II, together with the world averaged values [3], and Q_h [= $\mathcal{B}(\psi(2S) \rightarrow h)/\mathcal{B}(J/\psi \rightarrow h)$].

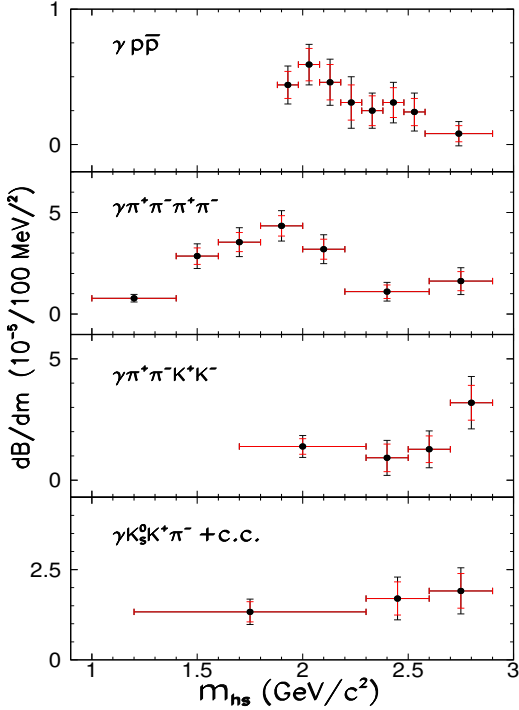


FIG. 3: Differential branching fractions for $\psi(2S)$ decays into $\gamma p\bar{p}$, $\gamma 2(\pi^+\pi^-)$, $\gamma K^+K^-\pi^+\pi^-$, and $\gamma K_S^0 K^+\pi^- + c.c.$. Here m_{hs} is the invariant mass of the hadrons in each final state. For each point, the smaller vertical error is the statistical error, while the bigger one is the sum of statistical and systematic errors.

Table III lists the sources of the systematic errors on the branching fractions. The systematic error caused by MDC tracking and the kinematic fit is estimated by using simulations with different MDC wire resolutions [6]. The systematic errors on photon and charged particle identification are taken as 2% per photon [6] and 2% per charged particle [6], respectively. The difference of the fit to the χ^2_{4C} distribution between MC simulation and data for $\psi(2S) \rightarrow \gamma \chi_{c0}$, $\chi_{c0} \rightarrow \text{hadrons}$ is about 3%, which is taken as the systematic error of the χ^2 fit method. The uncertainty of the total number of $\psi(2S)$ events is 4% [13], the uncertainty of the background estimation varies from 1-25% depending on the channel and background level, and the uncertainties of the branching fractions used are taken from Ref. [3]. Adding up all these sources in quadrature, the total systematic errors range from 7 to 28% depending on the channel.

In Fig. 3, broad peaks appear in the $m_{p\bar{p}}$ and $m_{4\pi}$ distributions at masses $1.9-2.5$ GeV/c^2 and $1.4-2.2$ GeV/c^2 , respectively, which are similar to those observed in J/ψ decays into the same final states [11, 14]. The possible structure within these broad peaks cannot be resolved with our samples. No obvious structure is observed in the other final states with the current statistics. The branching fractions below $m_{hs} < 2.9$ GeV/c^2 in this Letter sum up to 0.26% [15] of the total $\psi(2S)$ decay width, which is about a quarter of the total expected

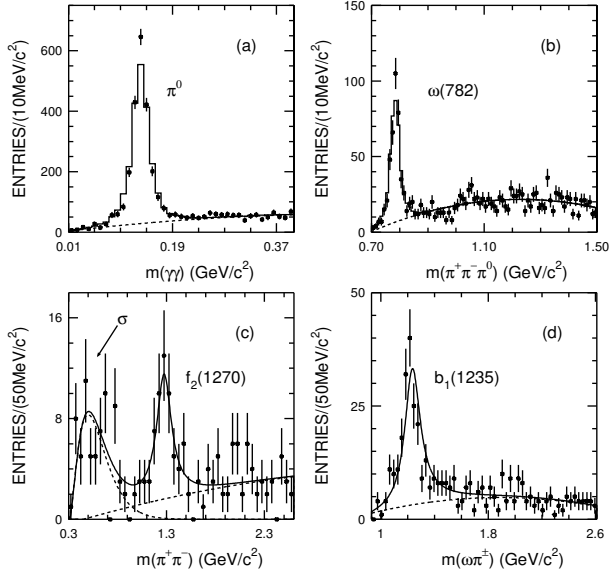


FIG. 4: Invariant mass distributions with fits for $\psi(2S) \rightarrow \pi^0 2(\pi^+ \pi^-)$, where dots with error bars are data; the solid histograms and curves denote the fit results. (a) $\gamma\gamma$; (b) $\pi^+ \pi^- \pi^0$ with $|m_{\gamma\gamma} - 0.135| < 0.03$ GeV/c^2 ; (c) $\pi^+ \pi^-$ with $|m_{\pi^+ \pi^- \pi^0} - 0.782| < 0.05$ GeV/c^2 ; and (d) $\omega \pi^\pm$ with $\omega f_2(1270)$ events removed for the $\psi(2S) \rightarrow \pi^0 2(\pi^+ \pi^-)$ candidate events. Resonance parameters are fixed to their world averaged values [3].

radiative $\psi(2S)$ decays. This indicates that a larger data sample is needed to search for more decay modes and to resolve the substructure of the $\psi(2S)$ radiative decays.

In summary, we report first measurements of the branching fractions of $\psi(2S)$ decays into $\gamma p\bar{p}$, $\gamma 2(\pi^+ \pi^-)$, $\gamma K_S^0 K^+ \pi^- + c.c.$, $\gamma K^+ K^- \pi^+ \pi^-$, $\gamma K^{*0} K^- \pi^+ + c.c.$, $\gamma K^{*0} \bar{K}^{*0}$, $\gamma \pi^+ \pi^- p\bar{p}$, $\gamma 2(K^+ K^-)$, $\gamma 3(\pi^+ \pi^-)$, and $\gamma 2(\pi^+ \pi^-) K^+ K^-$, and the differential branching fractions for $\psi(2S)$ decays into $\gamma p\bar{p}$, $\gamma 2(\pi^+ \pi^-)$, $\gamma K^+ K^- \pi^+ \pi^-$, and $\gamma K_S^0 K^+ \pi^- + c.c.$ with m_{hs} less than 2.9 GeV/c^2 . The branching fractions for $\psi(2S)$ decays into $\pi^0 2(\pi^+ \pi^-) K^+ K^-$ are measured for the first time. The measurements of $\psi(2S)$ decays into $\pi^0 2(\pi^+ \pi^-)$, $\omega \pi^+ \pi^-$, $\omega f_2(1270)$, and $b_1^\pm \pi^\mp$ are consistent with the recent measurements by the CLEO collaboration [16] and previous measurements [3].

The BES collaboration thanks the staff of BEPC and computing center for their hard efforts. This work is supported in part by the National Natural Science Foundation of China under contracts Nos. 10491300, 10225524, 10225525, 10425523, 10625524, 10521003, the Chinese Academy of Sciences under contract No. KJ 95T-03, the 100 Talents Program of CAS under Contract Nos. U-11, U-24, U-25, and the Knowledge Innovation Project of CAS under Contract Nos. U-602, U-34 (IHEP), the National Natural Science Foundation of China under Contract No. 10225522 (Tsinghua University), and the Department of Energy

TABLE II: Results of $\psi(2S) \rightarrow \pi^0 + \text{hadrons}$. Here N^{Sig} is the number of signal events, ϵ is the detection efficiency, \mathcal{B} is the measured branching fraction, \mathcal{B}^{PDG} is the world averaged value, and Q_h is defined in the text.

| Mode: h | N^{Sig} | $\epsilon(\%)$ | $\mathcal{B}(\times 10^{-4})$ | $\mathcal{B}^{\text{PDG}}(\times 10^{-4})$ | $Q_h(\%)$ |
|--------------------------------|---------------|----------------|-------------------------------|--|----------------|
| $\pi^0 2(\pi^+ \pi^-)$ | 2173 ± 53 | 6.32 | $24.9 \pm 0.7 \pm 3.6$ | 23.7 ± 2.6 | 10.5 ± 2.0 |
| $\omega \pi^+ \pi^-$ | 386 ± 23 | 3.74 | $8.4 \pm 0.5 \pm 1.2$ | 6.6 ± 1.7 | 11.7 ± 2.4 |
| $\omega f_2(1270)$ | 57 ± 13 | 3.65 | $2.3 \pm 0.5 \pm 0.4$ | 2.0 ± 0.6 | 5.4 ± 0.6 |
| $b_1^\pm \pi^\mp$ | 202 ± 21 | 3.24 | $5.1 \pm 0.6 \pm 0.8$ | 3.6 ± 0.6 | 17.0 ± 4.2 |
| $\pi^0 2(\pi^+ \pi^-) K^+ K^-$ | 65 ± 17 | 0.46 | $10.0 \pm 2.5 \pm 1.8$ | — | — |

TABLE III: Summary of the systematic errors.

| Source | Uncertainty |
|-------------------------|-------------|
| Wire resolution | 5-14% |
| Photon detection | 2%/photon |
| Particle identification | 2%/track |
| Signal fit | 3% |
| Background estimation | 1-25% |
| Number of $\psi(2S)$ | 4% |
| Intermediate states | 1-3% |
| Total | 7-28% |

under Contract No.DE-FG02-04ER41291 (U. Hawaii).

[1] L. Köpke and N. Wermes, Phys. Rep. **174**, 67 (1989).
[2] N. Brambilla *et al.*, CERN-2005-005, hep-ph/0412158.
[3] Particle Data Group, W.-M. Yao *et al.*, J. Phys. G **33**, 1 (2006).
[4] P. Wang, C. Z. Yuan, and X. H. Mo, Phys. Rev. D **70**, 114014 (2004).
[5] BES Collaboration, J. Z. Bai *et al.*, Nucl. Instr. Meth. A **458**, 627 (2001).
[6] BES Collaboration, M. Ablikim *et al.*, Nucl. Instrum. Meth. A **552**, 344 (2005).
[7] BES Collaboration, M. Ablikim *et al.*, Phys. Rev. D **71**, 072006 (2005).
[8] BES Collaboration, M. Ablikim *et al.*, Phys. Rev. D **73**, 052004 (2006).
[9] J. C. Chen *et al.*, Phys. Rev. D **62**, 034003 (2000).
[10] R. G. Ping *et al.*, High Energy Phys. Nucl. Phys. **31**, 229 (2007) [arXiv:physics/0608213].
[11] BES Collaboration, M. Ablikim *et al.*, Phys. Rev. Lett. **91**, 022001 (2003).
[12] The $p\bar{p}$ mass resolution in the fitted region is less than $3 \text{ MeV}/c^2$ and neglected in the fit.

- [13] X. H. Mo *et al.*, High Energy Phys. Nucl. Phys. **27**, 455 (2004) [arXiv:hep-ex/0407055].
- [14] D. Bisello *et al.*, Phys. Rev. D **39**, 701 (1989); R. M. Baltrusaitis *et al.*, Phys. Rev. D **33**, 1222 (1986).
- [15] This value includes the decays of $\psi(2S) \rightarrow \gamma\pi^+\pi^-\pi^0\pi^0$, $\gamma K^0\bar{K}^0 + c.c.$; the intermediate resonance channels, e.g. $\psi(2S) \rightarrow \gamma K^{*0}\bar{K}^{*0}$ are excluded.
- [16] CLEO Collaboration, R. A. Briere *et al.*, Phys. Rev. Lett. **95**, 062001 (2005).